Journal of Statistical Physics, Vol. 20, No. 3, 1979

Adsorption of Dipolar Hard Spheres onto a Smooth, Hard Wall in the Presence of an Electric Field

D. J. Isbister[1] and B. C. Freasier[1]

Received July 11, 1978

Integral equations have been solved for the density profile of dipolar hard spheres against a hard, smooth wall in the presence of an electric field. This density profile was examined as a function of the bulk medium's temperature and density with different field strengths and field directions. It was found to depend primarily upon the competitive interactions of the field with the monolayer particles and the first outer shell with the monolayer particles.

KEY WORDS: Mean spherical approximation; adsorption; applied field; dipolar fluid; Baxter's method; surface phenomena.

1. INTRODUCTION

Some of the most provocative problems in theoretical physics arise from the study of inhomogeneous systems. Unfortunately, as often as not, these are also some of the more difficult problems to solve analytically. For some time, integral equations have been used to study homogeneous fluids (constant density) with a fair degree of success. In fact, with certain closure conditions it has been possible to solve these integral equations (generally, the Ornstein–Zernike—OZ—equation) for a number of simple (but nontrivial) pair potentials.[1] Study of the solution of these equations has stimulated a large amount of thought into the nature of the local structure in liquids, and these solutions often agree qualitatively with direct machine simulations.[1]

One of the inhomogeneous problems of great interest in liquid state physics concerns the behavior of a fluid against a wall. A simple description of the thermodynamic behavior of hard spheres in contact with a wall was

Supported by the ARGC.

[1] Department of Chemistry, University of New South Wales, Royal Military College, Duntroon, Australia.

0022-4715/79/0300-0331$03.00/0

developed by Reiss *et al.*[2] These workers originally interpreted a wall as the result of the growth of a particular isolated particle, with the thermodynamic behavior being given by the associated limits of the equations arising out of scaled particle theory. Recently several publications[3–6] have given the microscopic properties of inhomogeneous systems by taking judicious limits of the solution to the OZ equation for mixtures with hard cores. Perram and Smith[3] specifically studied these limits in mixtures of "sticky" spheres. They were able to produce density profiles against the wall whose qualitative structure has since been confirmed by simulation results for other, more realistic model potentials.[7,8]

Isbister[9] has solved the two-component dipolar hard-sphere problem in the mean spherical approximation. It turns out that in addition to taking the density and radius limit of one component to produce the wall, it is also possible to produce an electric field if the polarity of that same component is held constant. In the next section we will present the appropriate details of the two-component dipolar hard-sphere problem, the mechanics of the hard-wall limit, and the mechanics of the polarization limit. In Section 3, we shall first graphically present density profiles against the wall for various dipole orientation and electric field angles. We shall then discuss in detail the competitive interactions which determine the monolayer (contact) density profile for this model. Finally, we shall make some brief comments on future extensions of this model.

2. DENSITY PROFILES: A STATISTICAL MECHANICAL APPROACH

Physical adsorption density profiles near a smooth, hard wall can be treated within the framework of liquid state models appropriate to a statistical mechanical approach. The foundations of such an approach were given by the pioneering work of Perram and Smith.[3] Their physical arguments for the use of certain limiting processes have been further strengthened by the recent results of Percus[4] (using functional analysis techniques). The basic concept in the Perram–Smith approach is the interpretation of the number density of α-species (of diameter R_α) particles at a distance r from a particle of different species β (of diameter R_β) fixed at the origin $\rho_\alpha(r)$. It is well known from mixture theories in statistical mechanics that the quantity $\rho_\alpha(r)$ is equivalent to the total correlation function $h_{\alpha\beta}(r)$ describing the radial dependence of the α–β species–species correlations. Specifically, $\rho_\alpha(r)$ is given in terms of $h_{\alpha\beta}(r)$ and the bulk density of species α, ρ_α, by

$$\rho_\alpha(r) = \rho_\alpha[h_{\alpha\beta}(r) + 1] \tag{2.1}$$

If an isolated particle of species β is allowed to increase its size indefi-

nitely, the quantity $\rho_\alpha(r)$ will then describe the local density of particles of species α at a distance $r - R_\beta/2$ away from a wall. In other words, the density profiles of each species α from a wall are described by the limiting behavior of $h_{\alpha\beta}(r)$ as ρ_β tends to zero and R_β to infinity (in that order):

$$\rho_\alpha(r) = \lim_{R_\beta \to \infty} \left\{ \lim_{\rho_\beta \to 0} \rho_\alpha [h_{\alpha\beta}(r) + 1] \right\} \tag{2.2}$$

Applications of Eq. (2.2) to physisorption have used spherically symmetric interaction potentials in modeling the mixture whose limiting behavior, as described in Eq. (2.2), is to be determined. In this section, we shall employ the limiting procedures detailed in Eq. (2.2) to describe the angular and spatial correlations of a fluid near a wall where the particle–particle interactions in the fluid bulk are nonspherically symmetric. Specifically, the system of interest exhibiting such an isotropy is modeled by mixtures of dipolar hard spheres. Fortunately, the structural and thermodynamic properties of mixtures of dipolar hard spheres have been calculated within the mean spherical approximation.[10,11] Despite certain quantitative inadequacies of the mean spherical approximation, the qualitative behavior is correct.[12] Coupled to the reduction of the problem to analytic form, and given the well-established procedures of Stell and co-workers[13] to correct basic inadequacies of the model, it would be desirable to use the structural behavior of dipolar hard spheres (within the mean spherical approximation) as at least a reference system. The structural properties predicted by such a reference system should not only be qualitatively correct, but also could be successively corrected (for example, by the generalized mean spherical approximation initially) to a level where comparisons to experimental or computer results would be meaningful.

For a binary mixture of dipolar hard spheres the density profile of pure species ($\alpha = 1$) becomes a function not only of the separation from the wall ($\beta = 2$), $r - \frac{1}{2}R_2$, but also of the angular configurations of the dipole directions $\mathbf{\Omega}_i = (\theta_i, \phi_i)$, $i = 1, 2$. In particular, Eq. (2.2) becomes

$$\rho_1(\mathbf{r}_{12}, \mathbf{\Omega}_1, \mathbf{\Omega}_2) = \lim_{R_2 \to \infty} \left\{ \lim_{\rho_2 \to 0} (\rho_1/4\pi)[h_{12}(\mathbf{r}_{12}, \mathbf{\Omega}_1, \mathbf{\Omega}_2) + 1] \right\} \tag{2.3}$$

In Eq. (2.3), the directions $\mathbf{\Omega}_1$, $\mathbf{\Omega}_2$, and $\hat{\mathbf{r}}_{12} = \mathbf{r}_{12}/|\mathbf{r}_{12}|$ are defined with respect to a fixed Cartesian coordinate system S.

The total correlation functions $h_{\alpha\beta}(\mathbf{r}_{12}, \mathbf{\Omega}_1, \mathbf{\Omega}_2)$ ($\alpha, \beta = 1, 2$) are given by the solution of the Ornstein–Zernike equation:

$$h_{\alpha\beta}(\mathbf{r}_{12}, \mathbf{\Omega}_1, \mathbf{\Omega}_2) = c_{\alpha\beta}(\mathbf{r}_{12}, \mathbf{\Omega}_1, \mathbf{\Omega}_2) + \sum_{\gamma=1}^{2} \frac{\rho_\gamma}{4\pi} \int d\mathbf{r}_3 \int d\mathbf{\Omega}_3 \times c_{\alpha\gamma}(\mathbf{r}_{13}, \mathbf{\Omega}_1, \mathbf{\Omega}_3) h_{\gamma\beta}(\mathbf{r}_{32}, \mathbf{\Omega}_3, \mathbf{\Omega}_2) \tag{2.4}$$

where $c_{\alpha\beta}(\mathbf{r}_{12}, \Omega_1, \Omega_2)$ is the direct correlation function for the α–β species interaction. Equation (2.4) is closed by the mean spherical approximation, which gives the following boundary conditions:

$$h_{\alpha\beta}(\mathbf{r}_{12}, \Omega_1, \Omega_2) = -1 \qquad \text{if} \quad r_{12} < R_{\alpha\beta} \tag{2.5}$$

and

$$c_{\alpha\beta}(\mathbf{r}_{12}, \Omega_1, \Omega_2) = -v_{\alpha\beta}(\mathbf{r}_{12}, \Omega_1, \Omega_2)/kT \qquad \text{if} \quad r_{12} > R_{\alpha\beta} \tag{2.6}$$

where $r_{12} = |\mathbf{r}_{12}|$. In Eqs. (2.5)–(2.6), k is the Boltzmann constant, T is the absolute temperature, and $R_{\alpha\beta}$ and $v_{\alpha\beta}$ are defined by

$$R_{\alpha\beta} = (R_\alpha + R_\beta)/2 \tag{2.7}$$

and $v_{\alpha\beta}(\mathbf{r}_{12}, \Omega_1, \Omega_2)$ is the dipolar part of the dipolar hard-sphere potential $\mathbf{u}_{\alpha\beta}(\mathbf{r}_{12}, \Omega_1, \Omega_2)$ defined in

$$u_{\alpha\beta}(\mathbf{r}_{12}, \Omega_1, \Omega_3) = u_{\alpha\beta}^{\mathrm{HS}}(r_{12}) + v_{\alpha\beta}(\mathbf{r}_{12}, \Omega_1, \Omega_2)$$

where

$$u_{\alpha\beta}^{\mathrm{HS}}(r_{12}) = \begin{cases} \infty & \text{if} \quad r_{12} < R_{\alpha\beta} \\ 0 & \text{if} \quad r_{12} > R_{\alpha\beta} \end{cases}$$

and

$$v_{\alpha\beta}(\mathbf{r}_{12}, \Omega_1, \Omega_2) = -(m_\alpha m_\beta / r_{12}^3)\mathbf{s}(\Omega_1)\cdot(3\hat{\mathbf{r}}_{12}\hat{\mathbf{r}}_{12} - \mathsf{U})\cdot\mathbf{s}(\Omega_2) \tag{2.8}$$

Here m_α is the dipole moment strength of a particle of species α, U is the unit dyadic in three-dimensional space, and $\mathbf{s}(\Omega_j)$ is the unit vector along the dipolar vector $\mathbf{m}_j$:

$$\mathbf{s}(\Omega_j) = (\sin\theta_j \cos\phi_j, \sin\theta_j \sin\phi_j, \cos\theta_j)$$

The substitution of the following invariant expansions for $h_{\alpha\beta}(\mathbf{r}_{12}, \Omega_1, \Omega_2)$ and $c_{\alpha\beta}(\mathbf{r}_{12}, \Omega_1, \Omega_2)$

$$\begin{aligned} h_{\alpha\beta}(\mathbf{r}_{12}, \Omega_1, \Omega_2) = {} & h_{\alpha\beta}^S(r_{12}) + h_{\alpha\beta}^\Delta(r_{12})\,\Delta(\Omega_1, \Omega_2, \hat{\mathbf{r}}_{12}) \\ & + h_{\alpha\beta}^D(r_{12}) D(\Omega_1, \Omega_2, \hat{\mathbf{r}}_{12}) \end{aligned} \tag{2.9}$$

$$\begin{aligned} c_{\alpha\beta}(\mathbf{r}_{12}, \Omega_1, \Omega_2) = {} & c_{\alpha\beta}^S(r_{12}) + c_{\alpha\beta}^\Delta(r_{12})\,\Delta(\Omega_1, \Omega_2, \hat{\mathbf{r}}_{12}) \\ & + c_{\alpha\beta}^D(r_{12}) D(\Omega_1, \Omega_2, \mathbf{r}_{12}) \end{aligned} \tag{2.10}$$

into Eq. (2.4) and the use of the constraints of Eqs. (2.5), (2.6), and (2.8) initiates the solution of the mean spherical approximation for dipolar hard-sphere mixtures.[14] It should be noted that the elements of the angular basis set are unity, Δ, and D, where Δ and D are defined by

$$\Delta(\Omega_1, \Omega_2, \hat{\mathbf{r}}_{12}) = \mathbf{s}(\Omega_1)\cdot\mathbf{s}(\Omega_2) \tag{2.11}$$

and

$$D(\Omega_1, \Omega_2, \hat{\mathbf{r}}_{12}) = \mathbf{s}(\Omega_1)\cdot(3\hat{\mathbf{r}}_{12}\hat{\mathbf{r}}_{12} - \mathsf{U})\cdot\mathbf{s}(\Omega_2) \tag{2.12}$$

The details of solution have been given elsewhere.[9] For completeness, a brief summary of the solution will be given below. It can be shown that the angular-dependent coupling in the Ornstein–Zernike equation [Eq. (2.4)] can be removed completely. The resulting three independent integral equations can be reduced to the Ornstein–Zernike equation for mixtures of hard spheres with mean spherical closure rules (equivalently, the Percus–Yevick closure rule) plus two other Ornstein–Zernike-like equations with unusual closure rules. Specifically, the spherical radial coefficient $h^S_{\alpha\beta}(r)$ is the usual Ornstein–Zernike equation with Percus–Yevick closure:

$$h^S_{\alpha\beta}(r_{12}) = c^S_{\alpha\beta}(r_{12}) + \sum_{\gamma=1}^{2} \rho_\gamma \int d\mathbf{r}_3\, h^S_{\alpha\gamma}(r_{13}) c^S_{\gamma\beta}(r_{32}) \tag{2.13}$$

where

$$h^S_{\alpha\beta}(r_{12}) = -1 \qquad \text{if} \quad r_{12} < R_{\alpha\beta}$$

and

$$c^S_{\alpha\beta}(r_{12}) = 0 \qquad \text{if} \quad r_{12} > R_{\alpha\beta} \tag{2.14}$$

The remaining equations are given in terms of the quantities $c^{\pm}_{\alpha\beta}(r)$, $h^{\pm}_{\alpha\beta}(r)$, and a self-consistently determined parameter $K_{\alpha\beta}$. These integral equations take the form of

$$h^{\pm}_{\alpha\beta}(r_{12}) = c^{\pm}_{\alpha\beta}(r_{12}) + \sum_{\gamma=1}^{2} \rho_\gamma{}^{\pm} \int d\mathbf{r}_3\, h^{\pm}_{\alpha\gamma}(r_{13}) c^{\pm}_{\gamma\beta}(r_{32}) \tag{2.15}$$

where $\rho_\gamma{}^{\pm}$ are defined by

$$\rho_\gamma{}^{\pm} = \begin{cases} 2\rho_\gamma & (+ \text{ case}) \\ -\rho_\gamma & (- \text{ case}) \end{cases}$$

The closure rules appropriate to Eq. (2.15) are

$$h^{\pm}_{\alpha\beta}(r) = -K_{\alpha\beta} \qquad \text{if} \quad r < R_{\alpha\beta}$$

and

$$c^{\pm}_{\alpha\beta}(r) = 0 \qquad \text{if} \quad r > R_{\alpha\beta} \tag{2.16}$$

where

$$K_{\alpha\beta} = \int_{R_{\alpha\beta}}^{\infty} dt\, t^{-1} h^D_{\alpha\beta}(t)$$

Equations (2.15)–(2.16) can be solved using Baxter's factorization technique[15] as originally formulated for Eqs. (2.13)–(2.14). Such an approach

gives the $h(^{\pm}_{\alpha\beta}r)$ in terms of $q^{\pm}_{\alpha\beta}(r)$, a known quadratic expression in r, in the following form:

$$rh^{\pm}_{\alpha\beta}(r) = -q'^{\pm}_{\alpha\beta}(r) + 2\pi \sum_{\gamma=1}^{2} \rho_\gamma{}^{\pm} \int_{S_{\alpha\gamma}}^{R_{\alpha\gamma}} dt\, q^{\pm}_{\alpha\gamma}(t)(r-t)h^{\pm}_{\gamma\beta}(|r-t|) \tag{2.17}$$

where

$$q^{\pm}_{\alpha\beta}(r) = \tfrac{1}{2}K_{\alpha\beta}a^{\pm}_{\alpha\beta}(r^2 - R^2_{\alpha\beta}) + K_{\alpha\beta}b^{\pm}_{\alpha\beta}(r - R_{\alpha\beta}), \quad S_{\alpha\beta} = \tfrac{1}{2}(R_\alpha - R_\beta) \tag{2.18}$$

and the $a^{\pm}_{\alpha\beta}$ and $b^{\pm}_{\alpha\beta}$ are known functions of the densities ρ_γ, diameters R_γ, and parameters $K_{\alpha\gamma}$. Finally, the anisotropic radial coefficients $h^{\Delta}_{\alpha\beta}(r)$ and $h^{D}_{\alpha\beta}(r)$ can be determined from the $h^{\pm}_{\alpha\beta}(r)$ by the following transformations; $h^{\Delta}_{\alpha\beta}(r)$ is a linear combination of $h^{\pm}_{\alpha\beta}(r)$:

$$h^{\Delta}_{\alpha\beta}(r) = 2[h^{+}_{\alpha\beta}(r) - h^{-}_{\alpha\beta}(r)] \tag{2.19}$$

while $h^{D}_{\alpha\beta}(r)$ is determined through an intermediate function $\hat{h}^{D}_{\alpha\beta}(r)$ in the following way:

$$\hat{h}^{D}_{\alpha\beta}(r) = 2h^{+}_{\alpha\beta}(r) + h^{-}_{\alpha\beta}(r) \tag{2.20}$$

and

$$h^{D}_{\alpha\beta}(r) = \hat{h}^{D}_{\alpha\beta}(r) - 3r^{-3}\int_0^r dt\, t^2 \hat{h}^{D}_{\alpha\beta}(t) \tag{2.21}$$

In summary, Eqs. (2.13), (2.15), and (2.19)–(2.21) can be used to obtain the radial coefficients appearing in the expression for $h_{\alpha\beta}(\mathbf{r}_{12}, \boldsymbol{\Omega}_1, \boldsymbol{\Omega}_2)$. Such a procedure is largely numerical and will not be presented in detail. However, it should be noted that the numerical determination of the parameters $K_{\alpha\beta}$ which effectively measure the long-range correlations in the mixture is done prior to the numerical solution of Eq. (2.17), i.e., the $q^{\pm}_{\alpha\beta}(r)$ are completely determined. The limiting behavior of these $h_{\alpha\beta}(\mathbf{r}, \boldsymbol{\Omega}_1, \boldsymbol{\Omega}_2)$ as described in Eq. (2.3) depends ultimately on the corresponding limiting behavior of the fundamental parameters $K_{\alpha\beta}$. Accordingly, attention will be given to the large-R_2, small-ρ_2 limiting behavior of the $K_{\alpha\beta}$.

In the limit of vanishingly small ρ_2 values the self-consistent equations which describe the $K_{\alpha\beta}$ as a function of the molecular parameters m_1, m_2, R_1, and R_2 and the macroscopic variables kT and ρ_1 take on a much simplified form [cf. Eqs. (3.5) of Ref. 9b, describing the ordinary mixture case]. An equation for K_{11} is found which is the result for the pure component case. In particular, K_{11} can be found through iteration of Eq. (2.22)[14]:

$$\tfrac{4}{3}\pi(m_1{}^2\rho_1/kT) = Q(2K_{11}\rho_1 R_1{}^3) - Q(-K_{11}\rho_1 R_1{}^3) \tag{2.22}$$

where $Q(x)$ is the inverse compressibility of a pure fluid of hard spheres in the Percus–Yevick approximation, i.e., $Q(x)$ is given by

$$Q(x) = (1 + 2x)^2/(1 - x)^4 \tag{2.23}$$

The determination of K_{12} is given in terms of K_{11} and m_2/R_{12}^3 through

$$m_1 m_2/kTR_{12}^3 = K_{12}[2Q(2K_{11}\rho_1 R_1{}^3) + Q(-K_{11}\rho_1 R_1{}^3)] \tag{2.24}$$

The limiting behavior of K_{22} is not required here since K_{11} and K_{12} are independent of K_{22}. It should be noted the value of K_{11} is independent of the size of R_2. In other words, the radial coefficients $h_{11}^S(r)$, $h_{11}^A(r)$, and $h_{11}^D(r)$ are independent of the presence of the infinitely dilute second component. Consequently the large-R_2 behavior of K_{12} need only be described.

If the limit as R_2 goes to infinity were directly applied to Eq. (2.24), K_{12} would approach zero as R_2^{-3}. In that limit, the anisotropic dependence of the correlation function $h_{12}(\mathbf{r}, \boldsymbol{\Omega}_1, \boldsymbol{\Omega}_2)$ disappears completely. Here the density profile of dipolar hard spheres away from the hard wall is purely determined by correlations induced by the hard-core repulsions of the dipolar hard sphere with the wall. Such hard-sphere, hard-wall density profiles have previously been generated using other methods.[3,5,16]

However, a more interesting limiting case is achieved if the dipole moment m_2 is allowed to grow in magnitude at a rate proportional to the excluded volume R_{12}^3. In this way, the ratio m_2/R_{12}^3 is finite, and as a consequence of Eq. (2.24), K_{12} is nonzero. This nonzero K_{12} ensures that through Eqs. (2.16)–(2.21) the anisotropic radial coefficients $h_{12}^A(r)$ and $h_{12}^D(r)$ are no longer trivially zero. Before discussing the density profiles [described through Eqs. (2.3) and (2.9)], it is appropriate to point out the physical interpretation of the constraint that m_2/R_{12}^3 be constant as ρ_2 goes to zero and R_2 to infinity.

The physical significance of finite values of the quantity m_2/R_{12}^3 is given in the limiting behavior of the dipole–dipole potential between any particle of species one interacting with the isolated particles of species two. If the distance between surfaces along the line of the intermolecular axis is defined as x, where $r_{12} = R_{12} + x$, by definition, then the limiting behavior of $v_{12}(\mathbf{r}_{12}, \boldsymbol{\Omega}_1, \boldsymbol{\Omega}_2)$ is given by Eq. (2.8) as

$$\begin{aligned}\lim_{R_2 \to \infty} v_{12}(\mathbf{r}_{12}, \boldsymbol{\Omega}_1, \boldsymbol{\Omega}_2) &= \lim_{R_2 \to \infty} \{-[m_1 m_2/(R_{12} + x)^3] D(\boldsymbol{\Omega}_1, \boldsymbol{\Omega}_2, \mathbf{r}_{12})\} \\ &= -m_1 \mathbf{s}(\boldsymbol{\Omega}_1) \cdot [(m_2/R_{12}^3)(3\hat{\mathbf{b}}\hat{\mathbf{b}} - \mathsf{U}) \cdot \mathbf{s}(\boldsymbol{\Omega}_2)] \end{aligned} \tag{2.25}$$

where $\hat{\mathbf{b}}$ is the limiting direction of $\hat{\mathbf{r}}_{12}$ for large R_2. Equation (2.25) can be rewritten in a form indicative of the electrostatic interaction of a dipole $\mathbf{m}_1$

[magnitude m_1 and direction $s(\Omega_1)$] with an external electric field $\mathbf{E}_0$. In other words, the limiting behavior of v_{12} in Eq. (2.25) is

$$\lim_{R_2 \to \infty} v_{12}(\mathbf{r}_{12}, \Omega_1, \Omega_2) = -m_1 s(\Omega_1) \cdot \mathbf{E}_0 \tag{2.26}$$

where the magnitude of $\mathbf{E}_0$ is

$$E_0 = m_2 f / R_{12}^3 \tag{2.27}$$

and direction

$$\hat{\mathbf{E}}_0 = \mathbf{f}/f \tag{2.28}$$

The vector $\mathbf{f}$ (of magnitude f) is defined by

$$\mathbf{f} = (3\hat{\mathbf{b}}\hat{\mathbf{b}} - \mathsf{U}) \cdot \mathbf{s}(\Omega_2) \tag{2.29}$$

From Eq. (2.29) the magnitude of $\mathbf{f}$ can be shown to be

$$f = \{3[\hat{\mathbf{b}} \cdot \mathbf{s}(\Omega_2)]^2 + 1\}^{1/2} \tag{2.30}$$

Equations (2.28)–(2.30) show that the resulting electrostatic field is not usually aligned with the direction of m_2, the magnitude of which determines the strength of the field through Eq. (2.27). In summary, the electrostatic field produced by the constraint that m_2/R_{12}^3 be finite is constant in magnitude and direction throughout the fluid.

From Eqs. (2.24)–(2.26) it follows that the quantity $m_1 m_2/(kTR_{12}^3)$ is proportional to the energy of interaction between a dipole in the fluid and the applied electrostatic field $\mathbf{E}_0$. Consequently the parameter K_{12} measures not only the short-range correlations in the fluid due to the presence of the wall, but also the long-range correlations in the fluid due to the aligning of molecules with the field. Incorporating the electrostatic field, Eq. (2.24) may be written as

$$K_{12} = \frac{E^*/T^*}{2Q(K_{11}\rho_1 R_1^3) + Q(-K_{11}\rho_1 R_1^3)} \tag{2.31}$$

where E^* and T^* are the reduced electrostatic field strength and temperature, respectively. These reduced variables are defined by

$$E^* = m_2 R_1^3 / m_1 R_{12}^3 f = E_0 R_1^3 / m_1 f \tag{2.32a}$$

$$T^* = kTR_1^3 / m_1^2 \tag{2.32b}$$

The factor of f appears in the denominator of Eq. (2.32a) because the magnitude of the field E_0 is dependent on the field's direction as well [see Eqs. (2.27)–(2.30)]. This basic anomaly is associated with the direction of the field being defined in terms of the dipole–dipole interaction tensor $3\hat{\mathbf{r}}_{12}\hat{\mathbf{r}}_{12} - \mathsf{U}$. However, the study of the density profile as a function of the

direction of the applied field for a given field strength can be made if the field strength is renormalized through Eqs. (2.30) and (2.32a).

Since the primary objective of this paper is to follow the effect of the field upon the density profiles, the numerical procedures used to obtain the radial coefficients in Eq. (2.9) should be mentioned. It is convenient to define $h^j(r)$ to be $h_{12}^S(r)$, $h_{12}^-(r)$, $h_{12}^+(r)$ for $j = 0, -, +$, respectively. In the limit of ρ_2 going to zero, Eq. (2.17) can be written for $r > R_{21}$ as

$$rh^j(r) = 2\pi {\rho_1}^j \int_0^{R_1} dt\, q_{11}^j(t)(r - t)h^j(|r - t|) \tag{2.33}$$

The general closure relations for the various $h^j(r)$ are compounded as

$$h^j(r) = -K^j \qquad \text{for} \quad r < R_{21} \tag{2.34}$$

where

$$K^0 = 1, \qquad K^+ = K^- = K_{12}, \qquad {\rho_1}^0 = \rho_1, \qquad {\rho_1}^+ = 2\rho_1,$$
$$\text{and} \qquad {\rho_1}^- = -\rho_1$$

The substitution $r = R_{21} + x$ into Eq. (2.33) followed by the taking of the second limit R_2 approaching infinity yields

$$h^j(R_{12} + x) = 2\pi {\rho_1}^j \int_0^{R_1} dt\, q_{11}^j(t)h^j(|R_{12} + x - t|) \tag{2.35}$$

Discretization of this integral equation in terms of the increment $\epsilon = R_1/N$ (ϵ was taken to be $R_1/20$ in the following calculations) and use of the trapezoidal rule to evaluate the convolution and of the identity $q_{11}^j(R_1) = 0$ gives[3]

$$[1 - \pi\epsilon {\rho_1}^j q_{11}^j(0)]h^j(R_{12} + m\epsilon)$$
$$= 2\pi {\rho_1}^j \epsilon \sum_{k=1}^{N-1} q_{11}^j(k\epsilon)h^j(R_{12} + (m - k)\epsilon) \tag{2.36}$$

In Eq. (2.36), q_{11}^j assumes the quadratic form

$$q_{11}^j(r) = K_{11}^j[\tfrac{1}{2}a_{11}^j(r^2 - {R_1}^2) + b_{11}^j(r - R_1)]$$

where

$$a_{11}^j = (1 + 2\xi^j)/(1 - \xi^j)^2, \qquad b_{11}^j = -\tfrac{3}{2}R_1\xi^j/(1 - \xi^j)^2$$

with

$$\xi^j = \tfrac{1}{6}\pi {\rho_1}^j K_{11}^j {R_1}^3$$

and $K_{11}^j = 1$, K_{11}, K_{11} for $j = 0, +, -$, respectively. The h^j as generated from Eq. (2.36) require the following initialization of the first $N + 1$ values of h^j:

$$h^j(k) = -K^j \qquad \text{for} \quad k = 1, 2, \ldots, N \tag{2.37}$$

and

$$h^j(N + 1) = \tfrac{1}{2}K^j\{[(1 + 2\xi^j)/(1 - \xi^j)^2] - 2\} \tag{2.38}$$

where

$$h^j(k) = h^j((k-1)\epsilon)$$

Finally, $h_{12}^{A}(r = R_{12} + m\epsilon)$ and $h_{12}^{D}(r = R_{12} + m\epsilon)$ are determined directly from Eqs. (2.19) and (2.20), respectively. The inversion of $\hat{h}_{12}^{D}(r)$ to obtain $h_{12}^{D}(r)$ is simplified in the limit of large R_2 to the following form:

$$h_{12}^{D}(r) = [2h_{12}^{+}(r) + h_{12}^{-}(r)] + 3K_{12} \tag{2.39}$$

Then the radial coefficients $h_{12}^{S}(r)$, $h_{12}^{A}(r)$, and $h_{12}^{D}(r)$ are stored for further evaluation at the various angular directions considered.

3. RESULTS

The density near the wall is given by Eq. (2.3) with (2.9). In Figs. 1–3 we have plotted $\rho_1(x, \mathbf{\Omega}_1, \mathbf{E}_0)/(\rho_1/4\pi)$, the density as a function of distance

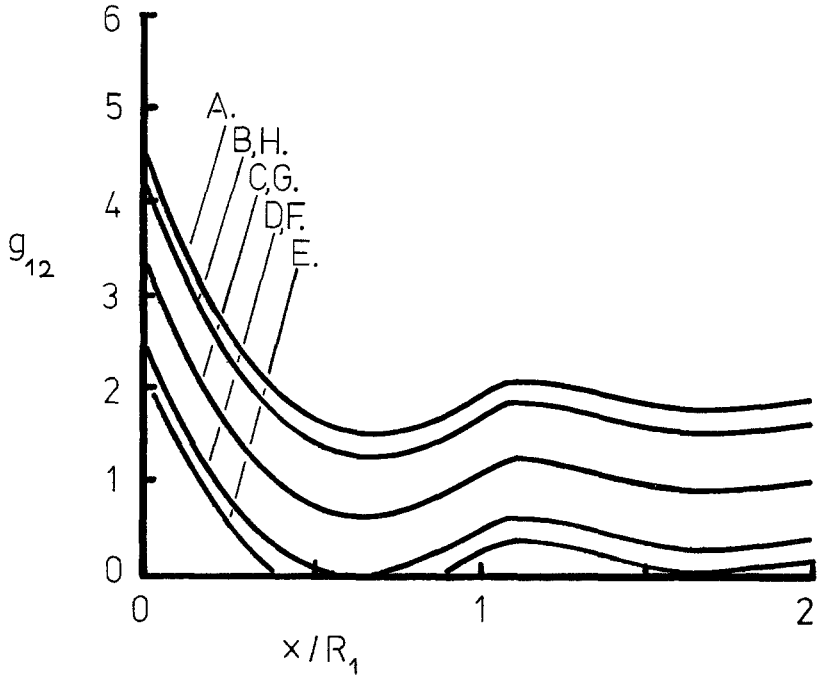

Fig. 1. Adsorption profiles as measured by $g_{12}(x) = 1 + h_{12}(R_{12} + x)$ for various dipole orientations when the bulk fluid parameters are $T^* = 2$ and $\chi = 0.3$. The various dipole orientational curves given by A–H represent $\theta_1 = 0$, $\pi/4$, $\pi/2$, $3\pi/4$, π, $5\pi/4$, $3\pi/2$, $7\pi/4$, respectively. The field strength is given by $E^* = 8/3$. The field angle θ_2 is zero.

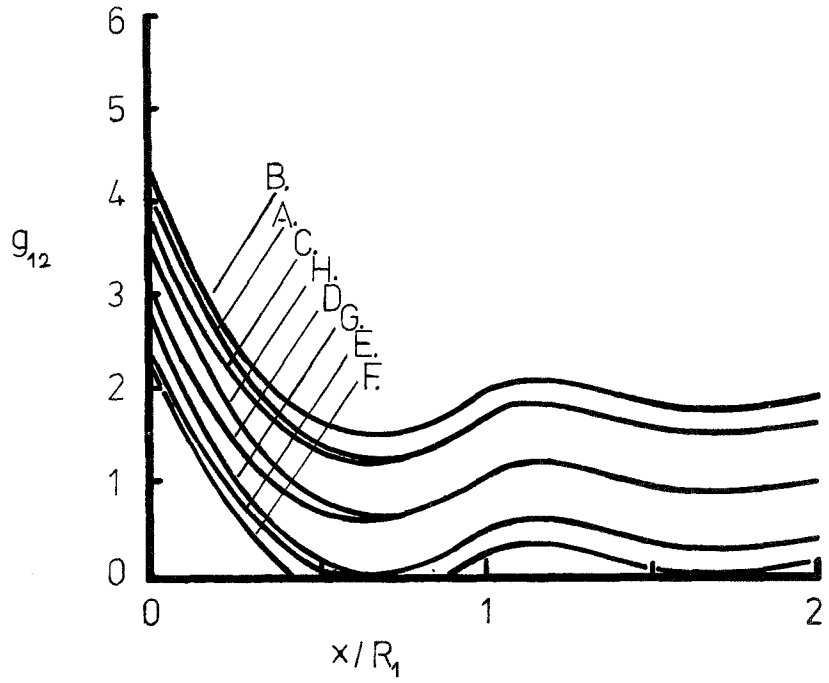

Fig. 2. Same as for Fig. 1 except that $\theta_2 = \pi/4$.

from the wall, for various field angles (0, 45, and 90° to the wall) and dipole angles (as defined in Fig. 4). From the figures it can be seen that the distribution can change as the distance from the wall increases, and the behavior near the wall requires separate consideration from behavior in the bulk of the fluid.

If we consider the Z axis to be perpendicular to the plane, the angles of interest are given in Fig. 4. The field angle and dipole angle are coplanar, with the azimuthal angle set equal to zero.

We refer to the region adjacent to the wall to the first minimum of ρ as the monolayer, and the region to the second minimum of ρ as the first outer shell. The contact value of the density function can be regarded as a quantitative measure of the physisorption in the monolayer.

3.1. Bulk Behavior

In considering these figures it should be noted that in the bulk region the behavior of the density function is determined by h_{12}^{D},[14] which is non-

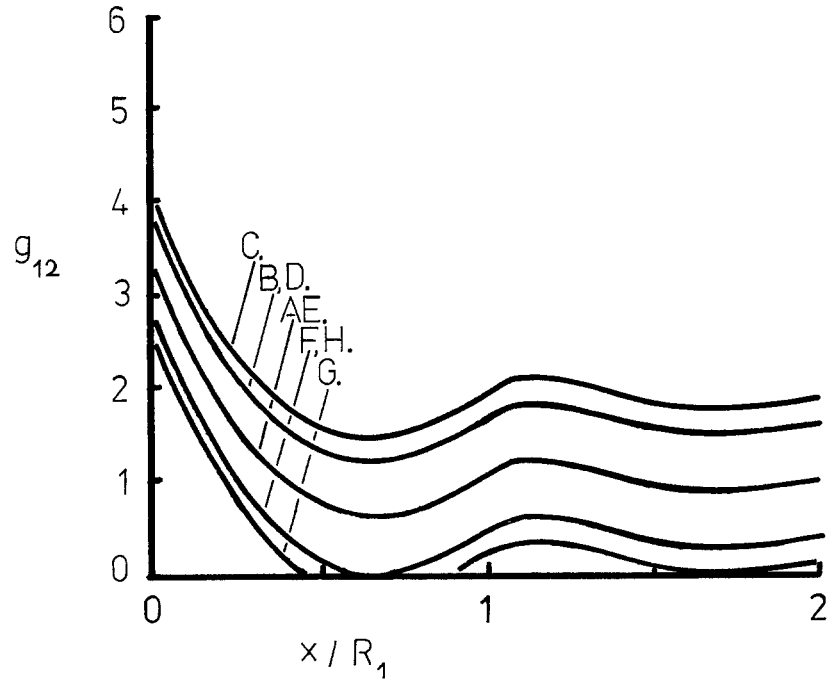

Fig. 3. Same as for Fig. 1 except that $\theta_2 = \pi/2$.

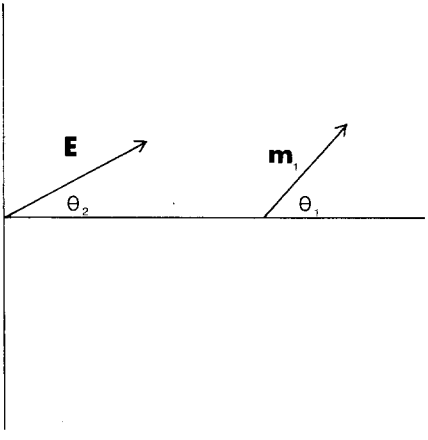

Fig. 4. The angle that the field **E** makes with the vector perpendicular with the wall is θ_2. The angle that the dipole moment $\mathbf{m}_1$ makes with the vector perpendicular to the wall is given by θ_1. Note that θ_1 and θ_2 are taken to be coplanar, with the azimuthal angle equal to zero.

zero. Specifically in Eq. (2.39), h_{12}^{+} and h_{12}^{-} approach zero as r becomes large, so that in the bulk region

$$h_{12}^{D}(r) = 3K_{12} \tag{3.1}$$

If we combine this result with the fact that h_{12}^{S} goes to zero and with Eq. (2.31), we obtain the following asymptotic behavior for the density profile:

$$\rho_1(\boldsymbol{\Omega}_1, \mathbf{E}_0) = \frac{\rho_1}{4\pi}\left\{1 + \frac{3E^*/T^* D(\boldsymbol{\Omega}_1, \boldsymbol{\Omega}_2, \hat{\mathbf{r}}_{12})}{2Q(2K_{11}\rho_1 R_1^3) + Q(-K_{11}\rho_1 R_1^3)}\right\}$$

$$= \frac{\rho_1}{4\pi}\left\{1 + \frac{3\mathbf{E}_0 \cdot \mathbf{m}_1}{kT[2Q(2K_{11}\rho_1 K_1^3) + Q(-K_{11}\rho_1 R_1^3)]}\right\} \tag{3.2}$$

This result differs from the first-order result (from expanding $\exp(\beta \mathbf{E}_0 \cdot \mathbf{m}_1)$ and averaging in the zero-field ensemble) by the compressibility factors in the denominator of Eq. (3.2). In fact, from Eq. (3.2) it is easy to see that the orientational ordering in the bulk will mimic the energetics of the dipole–electric field interaction, since the Q factors do not depend upon orientation.

For example, in Fig. 1, one can see that the ordering of the probabilities of the dipole orientation can be explained on the basis of the value of $\mathbf{E}_0 \cdot \mathbf{m}_1$. The most preferred orientation is parallel to the field and the least preferred is antiparallel to the field, with the other orientations distributed according to Eq. (3.2). Similar behavior is found in Figs. 2 and 3 when the field angle is changed. The relatively large field splitting in the bulk is due to the fact that the dipolar-field interaction is typically two to three times greater than the dipole–dipole interaction at contact. The field–dipole interaction can be measured by E^*/T^*, and the dipole–dipole interaction strength can be measured by $1/T^*$. In our case we took $E^* = 8/3$ and $T^* = 2$, giving a relative strength of 8/3.

3.2. Wall Behavior

Generally, for the cases we have considered the relative orientational order in the first outer shell is the same as for the bulk (see Figs. 1–3). In other words, the relative populations in the first outer shell and beyond are largely determined by the electric field–dipole interaction. An interesting effect occurs in the monolayer, however. In this region it is possible to have competitive interaction of the dipoles in the monolayer with the first outer shell, and the dipoles in the monolayer with the field. If the field angle is zero (Fig. 1), the two interactions are complementary, so that the bulk ordering persists to the monolayer. In this case the ordering of the dipoles in the monolayer due to the electric field is reinforced by the most populated

orientational states in the first outer shell. On the other hand, for other field angles (Figs. 2–3), orientations energetically favored by the field may not be favored by the dipole–dipole interactions. All of the splittings in the figures can be understood in terms of this competitive process. Consider Fig. 2, where the field angle is $\pi/4$. The favored orientation in the bulk (and the first outer shell) is parallel to the field ($\pi/4$). If the field completely determined the structure in the monolayer, then these particles would be similarly aligned. However, the monolayer dipole–first outer shell dipole interaction for two particles with alignment $\pi/4$ is not the most energetically favored. In fact, the most favored monolayer–first outer shell dipolar interaction is when the monolayer particle is set at $7\pi/4$ rad. Consequently, the monolayer density for $7\pi/4$ increases out of all proportion with respect to the bulk ordering. It is still very much a competitive process, for one can see that the most favored monolayer configuration is for $\pi/4$ radians, which combines strongly favored field–dipole and dipole–dipole interactions. Similar comments apply to Fig. 3 with respect to the comparison of the relative population of the monolayer orientation to that of the bulk.

We have presented the results for a single bulk density and bulk temperature ($\frac{1}{6}\pi\rho_1 R_1^3 = .3$, $kTR_1^3/m_1^2 = 2$). There are a few other trends that we shall remark upon briefly. As the field strength decreases, the bulk splitting becomes smaller and any degeneracies persist. There are also fewer particles in the monolayer. As the temperature decreases, there is greater adsorption in the monolayer, greater splitting in the bulk, and any splittings persist even to the extent of occurring outside the first outer shell. As the density decreases, the splittings become less prevalent because there are decreasing numbers of particles in the first outer shell to interact with the monolayer particles. In addition, the splitting in the bulk becomes larger as the field interactions in the bulk are less moderated by the dipole–dipole interaction.

4. CONCLUSIONS

We have shown that the method of Perram and Smith of examining a fluid near a wall may be extended in the case of dipolar hard spheres to allow consideration of a dipolar fluid in an electric field near a wall. The case of the electric field at a skewed angle with respect to a homogeneous wall will not ordinarily occur in nature, although there may be some heterogeneous surfaces for which the concept of a skewed field may be of value for certain axial configurations. In any event, the arbitrary field angle can be considered solely within the context of the model as an example of competitive adsorption due to the presence of an external potential which depends upon the orientation of the dipolar hard spheres in the bulk. We are not

unaware of the primitive nature of this model. Nevertheless, the model exhibits interesting competitive effects in adsorption. Further investigation is needed both of these angular effects and of the fluid–wall problem in general before quantitative comparison will be possible, but the fact that such a simple model exhibits qualitative features at all is encouraging, and suggests that extensions, for example, to competitive adsorption studies, may be very worthwhile.

ACKNOWLEDGMENTS

We would like to thank Dr. E. R. Smith for a very stimulating discussion, which initially interested us in this problem. We wish to thank Norm Hamer and Noel Thompson for several lengthy and constructive discussions concerning this manuscript. We would like to thank Prof. J. W. Perram for the use of a copy of his PY hard-sphere mixture program. We also thank Ms. Stella Quarry for her efforts and cooperation in typing the manuscript. Finally, we wish to acknowledge the ARGC for their support of this work.

REFERENCES

1. J. A. Barker and D. Henderson, *Rev. Mod. Phys.* **48**:587 (1976).
2. H. Reiss, H. L. Frisch, and J. L. Lebowitz, *J. Chem. Phys.* **31**:369 (1959); E. Helfand, H. Reiss, H. L. Frisch, and J. L. Lebowitz, *J. Chem. Phys.* **33**:1379 (1960).
3. J. W. Perram and E. R. Smith, *Proc. R. Soc. Lond. A* **353**:193 (1977).
4. J. K. Percus, *J. Stat. Phys.* **15**:423 (1976).
5. D. Henderson, F. F. Abraham, and J. A. Barker, *Mol. Phys.* **31**:1291 (1976); **32**:1785 (1976).
6. L. Blum and G. Stell, *J. Stat. Phys.* **15**:439 (1976).
7. F. F. Abraham, D. E. Schreiber, and J. A. Barker, *J. Chem. Phys.* **62**:1958 (1975).
8. G. A. Chapela, G. Saville, and J. S. Rowlinson, *J. Chem. Soc. Faraday Division, Gen. Disc.* **59**:22 (1975).
9. (a) D. Isbister and R. J. Bearman, *Mol. Phys.* **28**:1297 (1974); (b) *Mol. Phys.* **32**:597 (1976); (c) D. Isbister, *Mol. Phys.* **32**:949 (1976).
10. B. C. Freasier and D. Isbister, to appear in *Mol. Phys.*
11. D. Isbister, B. C. Freasier, and R. J. Bearman, to be published.
12. H. C. Anderson, *Ann. Rev. Phys. Chem.* **26**:145 (1975).
13. J. S. Høye, J. L. Lebowitz, and G. Stell, *J. Chem. Phys.* **61**:3253 (1974); J. S. Høye and G. Stell, *J. Chem. Phys.* **67**:524 (1977); G. Stell and J. J. Weiss, *Phys. Rev. A* **16**:757 (1977).
14. M. S. Wertheim, *J. Chem. Phys.* **55**:4291 (1971).
15. R. J. Baxter, *J. Chem. Phys.* **52**:4559 (1970).
16. E. Waisman, D. Henderson, and J. L. Lebowitz, *Mol. Phys.* **32**:1373 (1976).